and of the arguments set out above. If $X_1(r,r_{13},r_{23},z)$ were known exactly, then these arguments would be exact. However, no exact values of I_2 appropriate to the square-mound potential are known so that any direct test of the success of our assumption that X_1 is a function of z alone is not, at present, possible. Indirect evidence in support of our present arguments is, then, valuable and can be sought in two directions.

The first concerns the calculations of paper I for the temperature-independent case of hard spheres where a direct test shows that the value of I_2 calculated on the assumption $X_1 =$ const is in error by about 2%. The inherent similarity between the hard-sphere and square-mound-potential functions would make it plausible that I_2 given by (20c) involves an error of a few percent. Because I_1, given by (18), is exact this would mean that $K(n)$ computed from Eq. (21) is more accurate than our present calculated I_2 itself.

The second indirect evidence suggesting a reasonable accuracy for our function I_2 comes from the calculated data for the fourth virial coefficient. For hard spheres, the value of D calculated under the assumption $X_1 =$ const is found to be about $\frac{1}{2}\%$ too high (see reference 3). For the present square-mound potential it has already been mentioned that the function D^M resulting from the present approach is virtually the same as the approximate function derived by Hiroike[6] using entirely different arguments. It is possible that both sets of data are quite wrong but, in this case, there is the problem of explaining why they are so remarkably alike.

The present arguments take the calculation of K only as far as the cube term in n, although in paper I the quartic term was also determined for hard spheres. The formulas developed above could, after rather tedious although elementary calculation, be extended to include higher powers in n. However, such an extension would, in this case, be very doubtful in the absence of a direct check on the accuracy of I_2 for the square-mound potential, which is, however, available for hard spheres. The inclusion of further terms must be associated with more information about the lower members of the set of functions X_i.

Electroelastic Properties of the Sulfides, Selenides, and Tellurides of Zinc and Cadmium*

Don Berlincourt, Hans Jaffe, and L. R. Shiozawa

Electronic Research Division, Clevite Corporation, Cleveland, Ohio

(Received 11 September 1962)

A complete set of elastic, piezoelectric, and dielectric constants is presented for the sulfides, selenides, and tellurides of zinc and cadmium. The piezoelectric constants for the hexagonal crystals in this group are markedly higher than for the cubic crystals. An elementary model theory applied to these data leads to electric charges on the metal atom increasing from $+0.066$ e for ZnTe to $+0.84$ e for CdS. The elastic compliance increases regularly with increasing anion and cation weight, with no break between the cubic and hexagonal crystals. Pyroelectric constants are given for CdS and CdSe. The quality factor of elastic resonances of CdS plates is measured as function of electric conductivity.

I. INTRODUCTION

THE binary compounds crystallizing in the tetrahedrally coordinated cubic sphalerite and hexagonal wurtzite structures are the simplest crystals lacking a center of symmetry and, hence, capable of exhibiting piezoelectric and related effects depending on polar symmetry. Compounds of the bivalent column II B metals, zinc and cadmium, and the bivalent column VI elements, sulfur, selenium, and tellurium, are stable to high temperatures and can be made sufficiently insulating to allow precise measurements of piezoelectric, elastic, and dielectric constants. Such data eventually may serve to verify a quantitative theory of piezoelectricity and elasticity in these structure types which have been of great interest since the earliest lattice theories of crystal elasticity.[1] Until recently, only cubic zinc sulfide crystals of natural origin were available for such measurements, but interest in semiconducting properties of II–VI compounds has led to growth processes yielding good crystals of most of these compounds. Piezoelectric[2-4]

---

[1] M. Born, *Atomtheorie des Festen Zustandes* (B. G. Teubner, Leipzig, 1923); also, M. Born and M. Goeppert-Mayer, in *Handbuch der Physik*, edited by S. Flügge (Verlag Julius Springer, Berlin, 1933), pp. 623–794.

[2] H. Jaffe, D. Berlincourt, and L. Shiozawa, Proceedings of the Fourteenth Annual Symposium on Frequency Control, U. S. Army Research and Development Laboratory, Fort Monmouth, New Jersey, 1960 (unpublished), p. 304.

[3] A. R. Hutson, Phys. Rev. Letters 4, 505 (1960).

[4] T. Tanaka and S. Tanaka, J. Phys. Soc. Japan 15, 726 (1960). The extremely low values found by these authors may be due to electric conductivity since they use a low-frequency method.

and elasti [2,5-7] constants of cadmium sulfide and the elastic constants of cadmium telluride[8] have already been reported. The present work[9,10] gives the first piezoelectric measurements on the selenides and tellurides of zinc and cadmium, and more complete data on cadmium sulfide, including the pyroelectric effect. For comparison, dynamic elastic and piezoelectric measurements were made on natural cubic zinc sulfide (sphalerite); the results agreed well with static measurements made more than 50 years[11] ago. Our results show a pronounced break in the level of piezoelectric effect between the hexagonal crystals CdS and CdSe, and the cubic crystals CdTe, ZnS, ZnSe, and ZnTe. We have not been able to obtain both cubic and hexagonal crystals of any single compound in adequate size or quality. The piezoelectric coupling between elastic and electric energy is of particular theoretical[12] and practical[13,14] interest in II–VI crystals, because their conductivity can be controlled. The attenuation of progressing elastic waves caused by such interaction has been reported.[15]

II. MEASUREMENT PROCEDURE

A. Preparation of Test Specimens

CdS, CdSe, and ZnTe crystals were grown from the vapor phase by a slightly modified Reynolds-Green[16,10] method. The CdS and CdSe crystals were grown from General Electric Company vacuum-purified, luminescent-grade powders. The ZnTe source material was prepared by reacting New Jersey Zinc Company "super-purity" Zn-11 with American Smelting and Refining Company "high-purity" tellurium. The normally n-type CdS and CdSe crystals were doped with approximately 10 ppm (parts per million) of copper acceptors, and the normally p-type ZnTe crystals were doped with 10 ppm of indium donors. The resistivities of these compensated crystals were increased further from 10^6–10^7 Ω cm to 10^9–10^{10} Ω cm by heating for 1 h at 700°C and quenching to room temperature. This

treatment tended to redissolve the compensating impurities that had partially precipitated during slow cooling of the original growth runs. Test specimens were sectioned from large, 25–100 g, single crystals by means of an abrasive-slurry band saw. Crystals were lapped with 3-μ garnet and lightly etched with HCl or 1:1 HNO$_3$ (for CdS–CdSe and ZnTe, respectively). Crystallographic orientation and dimensional orthogonality were held to a tolerance of $\pm 1°$. The specimen dimensions were held to a tolerance of less than $\pm 1\%$. Some of the ZnTe specimens contained one or more twins, but since the (111) twin composition planes were parallel to the electroded faces, and since the twinning operation is a rotation about the (111) axis normal to the composition plane, the measurements were not affected by their presence. The CdS and CdSe crystals were twin free. Crystals were electroded with air-drying silver paint or, in the case of ZnTe, an electroless gold coating.

ZnSe and CdTe crystals were obtained from the General Electric Company Research Laboratories through the courtesy of Manuel Aven and Max Lorenz, respectively. A natural ZnS crystal (sphalerite) (originating from Sonora, Mexico) of greenish-yellow to brown color in transmitted light was at hand. (111) plates were prepared from these crystals as described for ZnTe. A bar elongated in the [110] direction was cut from the ZnS crystal to allow a more accurate determination of the elastic constants.

B. Piezoelectric, Dielectric, and Elastic Measurements

Hexagonal Crystals

The measurement scheme is similar to the one used by two of the authors on barium titanate crystals[17] and followed resonance methods largely established by Mason,[18] supplemented by contour mode resonances of square plates.[19] The electroelastic tensor for the dihexagonal polar crystal class $(6mm = C_{6v})$ contains the following nonzero constants:

$$s_{11} = s_{22}, \; s_{33}, \; s_{12}, \; s_{13} = s_{23}, \; s_{44} = s_{55}, \; s_{66} = 2(s_{11} - s_{12});$$
$$d_{31} = d_{32}, \; d_{15} = d_{24}, \; d_{33};$$
$$\epsilon_{11} = \epsilon_{22}, \; \epsilon_{33}.$$

The following bars and plates were used: A, square plates perpendicular to the optic (c) axis; B, plates parallel to c; C, bars with length perpendicular to c, thickness parallel to c; D, bars with length at 30°, 45°, and 60° from c and width perpendicular to c. The plates were about 15 mm by 2 mm thick and the bars

[5] D. I. Bolef, N. T. Melamed, and M. Menes, J. Phys. Chem. Solids **17**, 143 (1960).

[6] H. J. McSkimmin, T. B. Bateman, and A. R. Hutson, J. Acoust. Soc. Am. **33**, 856 (1961).

[7] E. Gutsche, Physica Status Solidi **1**, 30 (1961).

[8] H. J. McSkimmin and D. G. Thomas, J. Appl. Phys. **33**, 56 (1962).

[9] A partial account was given at the American Physical Society Meeting, Monterey, California, March 1961. H. Jaffe, D. Berlincourt, and L. Shiozawa, Bull. Am. Phys. Soc. **6**, 139 (1961).

[10] Some of the present data and additional information on crystal growth and treatment are contained in L. R. Shiozawa *et al.*, U. S. Air Force Report ARL 62-365, 1962 (unpublished).

[11] W. G. Cady, *Piezoelectricity* (McGraw-Hill Book Company, Inc., New York, 1946), pp. 159, 229.

[12] A. R. Hutson, Suppl. J. Appl. Phys. **32**, 2287 (1961).

[13] A. R. Hutson, J. H. McFee, and D. L. White, Phys. Rev. Letters **7**, 237 (1961).

[14] D. L. White, J. Appl. Phys. **33**, 2547 (1962).

[15] H. D. Nine and R. Truell, Phys. Rev. **123**, 799 (1961).

[16] D. C. Reynolds and S. J. Czyzak, Phys. Rev. **79**, 543 (1950); L. C. Green, D. C. Reynolds, S. J. Czyzak, and W. M. Baker; J. Chem. Phys. **29**, 1375 (1958).

[17] D. Berlincourt and H. Jaffe, Phys. Rev. **111**, 143 (1958).

[18] W. P. Mason, *Piezoelectric Crystals and Their Application to Ultrasonics* (D. Van Nostrand Company, Inc., Princeton, New Jersey, 1950).

[19] IRE Standards on Piezoelectric Crystals: Determination of the Elastic, Piezoelectric, and Dielectric Constants—The Electromechanical Coupling Factor, 1958, Proc. Inst. Radio Engrs. **46** 765 (1958).

were about 20 mm long, 4 mm wide, and less than 1 mm thick.

The dielectric constants at constant stress ($\epsilon_{33}{}^T$ and $\epsilon_{11}{}^T$) were measured on A and B plates at 10 kc/sec in the dark. The dielectric constants at constant strain ($\epsilon_{33}{}^S$ and $\epsilon_{11}{}^S$) were measured at frequencies above the thickness extensional mode ($\epsilon_{33}{}^S$) or thickness shear mode ($\epsilon_{11}{}^S$) and its first five overtones.

The piezoelectric constants d_{31} or d_{31}' and the elastic constants $s_{11}{}^E$ or $s_{11}'{}^E$ were determined from the fundamental extensional mode of bars C and D. The elastic constant $s_{44}{}^D = 1/c_{44}{}^D$ was measured using overtones of the thickness shear mode of plates B with small circular driving electrodes. Harmonics up to the 25th were readily measured. In similar fashion, the elastic constant $c_{33}{}^D$ was obtained from overtones of the thickness extensional mode of plates A, and in this case harmonics up to the 17th were readily measured. The planar Poisson's ratio $-s_{12}{}^E/s_{11}{}^E$ was determined from the ratio of the resonance frequencies of the two fundamental extensional modes of plates A, and also from the ratio of the frequency constants of bars C and plates A. In each case the agreement was within 1.5%, and an average value was taken.

Rayleigh corrections to resonance frequencies were made for finite lateral dimensions of bars C and D, and all such corrections were less than 1%. A summary of directly measured values after Rayleigh correction is given in Table I. Results of static pressure tests used in determining the signs of piezoelectric constants are also summarized. The hydrostatic d constant ($d_h = 2d_{31} + d_{33}$) was measured using a calibrated hydrostatic stress. Within the resolution of the measurement, noted in Table I, $d_h = 0$. From the data listed in the Table the complete sets of elastic and piezoelectric constants are obtained by calculation.[17–19]

Cubic Crystals

Only one crystal specimen was necessary for the measurements on the cubic crystals, a square plate with surface perpendicular to [111]. Defining Z' parallel to [111] and X' parallel to [110], the piezoelectric constant d_{31}' was obtained from the resonance and antiresonance frequencies of the fundamental extensional mode.[19] The piezoelectric constant referred to the cubic axes is then given by

$$d_{14} = \sqrt{3}d_{33}' = -2\sqrt{3}d_{31}'. \tag{1}$$

The elastic constants $s_{11}'{}^E$ and $s_{12}'{}^E$ were obtained from the ratio of the resonance frequencies of the two fundamental planar extensional modes of the square plate, as with the hexagonal crystals. This is justified by planar isotropy about [111], since $s_{66}' = 2(s_{11}' - s_{12}')$. The elastic constant $c_{33}'{}^D$ was obtained from overtones of the thickness extensional mode of the plate. The elastic constants referred to cubic axes are then obtained by solution of the set of simultaneous equations below

TABLE I. Directly measured constants of cadmium sulfide and cadmium selenide bars and plates (25°C).

	CdS	CdSe
Elastic constants, s in 10^{-11} m²/N, c in 10^{10} N/m²		
$s_{11}{}^E$	2.069	2.338
$-s_{12}{}^E/s_{11}{}^E$	0.483	0.480
$s_{44}{}^D$	6.412	7.466
$c_{33}{}^D$	9.623	8.477
$s_{11}'{}^E(59°\ 25')$	...	2.350
$s_{11}'{}^E(29°\ 10')$	...	2.624
$s_{11}'{}^E(45°\ 30')$	2.356	...
$s_{11}'{}^E(29°)$	2.318	...
Dielectric constants		
$\epsilon_{33}{}^T/\epsilon_0$	10.33	10.65
$\epsilon_{11}{}^T/\epsilon_0$	9.35	9.70
$\epsilon_{11}{}^S/\epsilon_0$	9.02	9.53$_5$
$\epsilon_{33}{}^T/\epsilon_0(-196°C)$	9.48	...
$\epsilon_{11}{}^T/\epsilon_0(-196°C)$	8.48	...
Piezoelectric coupling factors		
k_{31}	0.119$_1$	0.083$_6$
$k_{31}'(59°\ 25')$	...	0.141
$k_{31}'(29°\ 10')$	...	0.027
$k_{31}'(45°\ 30')$	0.150$_3$	...
$k_{31}'(29°)$	0.0356	...

Additional measurements

$|d_h| < 0.05 \times 10^{-12}$ C/N (CdS and CdSe)
$d_{33} \sim +10^{-11}$ C/N (compression test, CdS and CdSe)
d_{31} negative (compression test, CdS and CdSe)
$d_{31}'(29°\ 10')$ positive (compression test, CdSe)
$d_{31}'(59°\ 25')$ positive (compression test, CdSe)
$d_{31}'(29°)$ positive (compression test, CdS)
$d_{31}'(45°\ 30')$ positive (compression test, CdS)

and the inversion relation of the c matrix.

$$c_{33}' = \tfrac{1}{3}(c_{11} + 2c_{12} + 4c_{44}),$$
$$s_{11}' = \tfrac{1}{4}(2s_{11} + 2s_{12} + s_{44}), \tag{2}$$
and
$$s_{12}' = \tfrac{1}{12}(2s_{11} + 10s_{12} - s_{44}).$$

Due to the low piezoelectric coupling of ZnTe, CdTe, and ZnSe, the difference between open-circuit and short-circuit elastic constants may be neglected. Directly measured data are summarized in Table II.

For ZnS a bar elongated along [110] with thickness parallel to [001] was used, as well as a square plate perpendicular to [111], allowing a more precise determination of the elastic constants. The elastic constants $s_{11}'{}^E$ and $s_{12}'{}^E$ were determined as with the cubic crystals, and $c_{44}{}^D = 1/s_{44}{}^D$ was determined from overtones of the thickness shear mode of the [110] bar (electrodes on end or edge faces). Directly measured data are listed in Table II.

The volume resistivity of the CdTe specimen was only $\sim 2 \times 10^5$ Ω cm at 25°C, increasing to $\sim 2 \times 10^9$ at -196°C. In view of this, the dielectric and piezoelectric measurements were made at -196°C. Measurements on ZnS were repeated at -196°C, and the low temperature d_{14} and e_{14} for CdTe were corrected to 25°C by arbitrarily applying the ratio between 25 and -196°C values of d_{14} and e_{14} obtained for ZnS. Directly measured data are listed in Table II.

TABLE II. Directly measured constants on cubic ZnS, ZnTe, ZnSe, and CdTe.

	ZnS (25°C)	ZnS (−196°C)	ZnTe (25°C)	ZnSe (25°C)	CdTe (−196°C)
Elastic constants, s in 10^{-11} m²/N, c in 10^{10} N/m²					
$s_{11}'^{E}$	1.108	1.087	1.566	1.275	2.405 (2.445) (at 25°C)
$-s_{12}'^{E}/s_{11}'^{E}$	0.414	0.416	0.380	0.407	0.458
$c_{33}'^{D}$	14.08	⋯	9.249	11.77	7.535
s_{44}^{D}	2.154	2.131	⋯	⋯	⋯
Dielectric constants					
$\epsilon_{11}'^{T}/\epsilon_0$	8.3$_7$	8.1$_4$	10.1$_0$	9.1$_2$	9.6$_5$
Piezoelectric constants, 10^{-12} C/N					
d_{31}'	0.91$_7$	1.00$_0$	0.26$_4$	0.31$_8$	0.48$_5$
Density, 10^3 kg/m³					
ρ	4.088	4.099^a	5.636	5.26$_2$	5.86

^{a} Corrected density assuming average thermal expansion of 4×10^{-6}/degC from −196 to 25°C.

C. Measurement of Pyroelectric Effects

The pyroelectric effects in hexagonal CdS and CdSe were measured by immersing plates A in liquid nitrogen. A capacitance of 1 μF was connected across the test specimen and an electronic electrometer was connected across this capacitor. The resistance of the test specimens was about 10^8 Ω at room temperature in the dark, and this resistance increases with decreasing temperature. The time constant was therefore greater than 100 sec, allowing sufficient time for temperature equilibrium.

D. Measurement of Open-Circuit Q of CdS with Varying Illumination Level

The effect of illumination-controlled conductivity on the mechanical quality factor Q_M of CdS was determined by measurement of the resonance and antiresonance resistances of bars C. With the fundamental relationship $Q = \omega U/P$, with U the averaged stored energy and P the power dissipated, it can be shown by standard equivalent circuits of piezoelectric crystals[20] that, in the presence of high conductive losses,

$$Q_{\text{MOC}} = \frac{\omega_a C^T k_m^2 (1 - k_m^2)(R_r R_0^2/X^2 + R_r + R_0)}{R_0^2/X^2 + 1 - k_m^2}, \quad (3)$$

where Q_{MOC} = open-circuit mechanical Q, R_r = resonance resistance measured in the dark, C^T = free capacitance measured in the dark, $k_m^2 = (\omega_a^2 - \omega_r^2)/\omega_a^2$ (measured in the dark), and $X = 1/\omega_a C^T(1 - k_m^2)$. R_0 in Eq. (3) actually represents the effective photoconductance at the antiresonance frequency. It is obtained by solution of the relationship below, with R_a the measured

[20] W. P. Mason, Proc. Inst. Radio Engrs. 23, 1252 (1935).

resistance at antiresonance.

$$R_a = \frac{X^2/R_r + R_0 + R_r}{X^2/R_0 R_r + 2 + R_r R_0/X^2 + R_r/R_0}. \quad (4)$$

The short-circuit mechanical Q is given by

$$1/Q_{\text{MSC}} = \omega_R R_r k_m^2 C^T. \quad (5)$$

For determination of Q_{MOC} the impedance at antiresonance Z_a was measured as a function of illumination. The illumination was provided by a tungsten projection lamp, the output of which first passed through a water cell and a glass filter in order to remove the infrared. The illumination was calibrated at two distances between the light source and the test element using a thermopile, which was placed at the position of the CdS bar. The illumination was varied by changing the distance between the test specimen and the light source. The test specimen was illuminated on the face perpendicular to its width. This face was about 3.1 mm by 20 mm and the width was 4.5 mm. The crystal was fairly clear and, therefore, quite transparent to visible light with wavelength over about 5200 Å.

III. RESULTS

A. Piezoelectric, Elastic, and Dielectric Data

Complete sets of piezoelectric, elastic, and dielectric constants for hexagonal CdS and CdSe are listed in

TABLE III. Elastic, dielectric, and piezoelectric constants of wurtzite CdS and CdSe, 25°C. s in 10^{-11} m²/N; d in 10^{-12} C/N; c in 10^{10} N/m²; e in C/m².

	CdS	CdSe		Inversion of s tensor CdS	CdSe	CdS^a
s_{11}^{E}	2.069	2.338	c_{11}^{E}	9.07	7.41	8.581
s_{33}^{E}	1.697	1.735	c_{33}^{E}	9.38	8.36	9.370
s_{12}^{E}	−0.999	−1.122	c_{12}^{E}	5.81	4.52	5.334
s_{13}^{E}	−0.581	−0.572	c_{13}^{E}	5.10	3.93	4.615
s_{44}^{E}	6.649	7.595	c_{44}^{E}	1.504	1.317	1.487
s_{66}	6.136	6.920	c_{66}	1.630	1.445	
s_{11}^{D}	2.040	2.322	c_{11}^{D}	9.13	7.42	
s_{33}^{D}	1.581	1.670	c_{33}^{D}	9.623	8.477	
s_{12}^{D}	−1.028	−1.138	c_{12}^{D}	5.88	4.53	
s_{13}^{D}	−0.523	−0.539	c_{13}^{D}	4.97	3.86	
s_{44}^{D}	6.412	7.466	c_{44}^{D}	1.560	1.340	
d_{31}	−5.18	−3.92	e_{31}	−0.244	−0.160	−0.244
d_{33}	+10.32	+7.84	e_{33}	+0.440	+0.347	+0.489
d_{15}	−13.98	−10.51	e_{15}	−0.210	−0.138	
k_{33}	0.262	0.194	$\epsilon_{33}^{T}/\epsilon_0=$	10.33	10.65	
k_{31}	0.119$_1$	0.083$_6$	$\epsilon_{11}^{T}/\epsilon_0=$	9.35	9.70	
k_{15}	0.188$_5$	0.130$_5$	$\epsilon_{11}^{S}/\epsilon_0=$	9.02	9.33	
k_t	0.154	0.124	$\epsilon_{33}^{S}/\epsilon_0=$	9.53	10.20	

Estimated accuracy (±)

	CdS	CdSe		CdS	CdSe		CdS	CdSe
$s_{11}^{E,D}$	0.2%	0.2%	d_{31}	2%	3%	ϵ_{33}^{T}	2%	2%
$s_{12}^{E,D}$	0.5%	0.5%	d_{33}	2%	3%	ϵ_{11}^{T}	2%	2%
$s_{44}^{E,D}$	0.2%	0.2%	d_{15}	4%	4%	$\epsilon_{11}^{S}/\epsilon_{11}^{T}$	0.5%	0.5%
c_{33}^{D}	0.2%	0.2%	k_{15}	3%	4%			
$s_{33}^{E,D}$	3%	1.0%	k_{31}	1%	2%			
$s_{13}^{E,D}$	5%	1.5%	k_{33}	4%	4%			
			k_t	4%	4%			

^{a} See reference 6.

TABLE IV. Temperature coefficients of elastic constants (not corrected for thermal expansion).

Elastic constant	Temperature coefficient at 25°C, 10^{-6}/°C
CdS	
s_{11}^E	+116
s_{12}^E	+87
c_{33}^D	−216
s_{44}^D	+96
ZnS	
	Average temperature coefficient −196 to 25°C, 10^{-6}/°C
$s_{11}'^E$	+98
$s_{12}'^E$	+78
s_{44}^D	+50
CdTe	
$s_{11}'^E$	+74

Table III. Estimated accuracy limits are noted for most of the constants. The directly measured piezoelectric and elastic tensors are those for d and s. With the exception of c_{33} and c_{44}, which were measured directly, error limits in the c matrix may be considerably higher; the c matrix of McSkimmin et al.[6] is, therefore, shown and used for calculation of preferred values for e_{33} and e_{31} of CdS ($e_{nj}=d_{ni}c_{ij}^E$).

Table IV shows temperature coefficients of several of the elastic constants of CdS at 25°C. In the temperature range −196 to 100°C the elastic constants change almost linearly, and the transverse coupling factor k_{31} remains constant at 0.119±0.001. The temperature coefficients of some of the elastic constants of ZnS and CdTe are also shown in Table IV. The temperature coefficients listed in the Table were not corrected for thermal expansion.

Complete sets of piezoelectric, elastic, and dielectric constants for cubic ZnS, ZnTe, ZnSe, and CdTe are shown in Table V. Error limits are also shown in Table V, and it is immediately evident that the errors in the elastic constants are relatively high for all except ZnS. The method of deriving a complete set of elastic constants from only one crystal plate, described in Sec. II B, involves a solution of a quadratic equation with near cancellation of terms. The extra bar used in the measurements on ZnS allows considerably higher accuracy. The higher error limits on the elastic compliance tensor for CdTe cause even larger errors in the elastic stiffness tensor (except c_{44}) and the agreement with reference 8 is only fair.

B. Pyroelectric Data

For CdS and CdSe the total changes of polarization from 25 to −196°C were 0.090 and 0.077 μC/cm^2, respectively. In both cases, that crystal face which becomes positive on extension (positive side of Z axis) is negative with increasing temperature, so the pyroelectric constant at constant stress $(\partial P/\partial\theta)_T$ is negative. If one assumes that the change in polarization is linear

with temperature in this range,[21] the pyroelectric coefficients $(\partial P/\partial\theta)_T$ are -4×10^{-4} and -3.5×10^{-4} μC/cm^2 °C for CdS and CdSe, respectively.

As noted, the pyroelectric measurements were made at constant stress, and piezoelectric charges due to thermal expansion were, therefore, included. The total pyroelectric effect in the temperature range −196 (θ_1) to 25°C (θ_2) is given by the following:

$$\Delta P_3(\text{constant stress}) = \Delta P_3(\text{constant strain})$$

$$+ \int_{\theta_1}^{\theta_2} (e_{33}\alpha_3 + 2e_{31}\alpha_1)d\theta, \quad (6)$$

where α_3, α_1 = thermal expansion coefficients parallel and perpendicular to c, respectively.

The integral in the equation above represents the secondary pyroelectric effect. Results shown in part A indicate that there is little variation with temperature of e_{33} or e_{31}. Thermal expansion coefficients have been determined only from 0 to 300°C. By extrapolation the average thermal expansion coefficients in the range −196 to 25°C are in 10^{-6}/°C: $\alpha_1=4.0$, $\alpha_3=2.1$ for CdS and $\alpha_1=4.4$, $\alpha_3=2.45$ for CdSe. Using these the secondary effects are −0.0204 and −0.0124 for CdSe, respectively,

TABLE V. Piezoelectric, elastic, and dielectric constants of cubic ZnS, ZnTe, ZnSe, CdTe. s in 10^{-11} m^2/N, c in 10^{10} N/m^2, d in 10^{-12} C/N, and e in C/m^2. s_{44}^E and s_{44}^D, c_{44}^E and c_{44}^D, ϵ_{11}^T and ϵ_{11}^S differ by less than 0.1% for ZnTe, ZnSe, and CdTe.

	ZnS (25°C)	ZnS (−196°C)	ZnTe (25°C)	ZnSe (25°C)	CdTe (−196°C)	CdTe[b] (25°C)
s_{11}	1.839	1.786	2.40	2.26	3.83	
s_{12}	−0.707	−0.685	−0.873	−0.85	−1.58	
s_{44}^E	2.168	2.148	3.21	2.27	5.11	
s_{44}^D	2.154	2.131	3.21	2.27	5.11	
c_{11}	10.46	10.71	7.13	8.10	6.15	5.351
c_{12}	6.53	6.67	4.07	4.88	4.30	3.681
c_{44}^E	4.613	4.655	3.12	4.41	1.96	1.994
c_{44}^D	4.643	4.693	3.12	4.41	1.96	
$\epsilon_{11}^T/\epsilon_0$	8.3$_7$	8.1$_4$	10.1$_0$	9.1$_2$	9.6$_5$	
$\epsilon_{11}^S/\epsilon_0$	8.3$_2$	8.0$_8$	10.1$_0$	9.1$_2$	9.6$_5$	
d_{14}	3.1$_8$	3.4$_6$	0.9$_1$	1.1$_0$	1.6$_8$[a]	
e_{14}	0.14$_7$	0.16$_2$	0.028$_4$	0.049	0.0335[a]	
k_{14}	0.079$_5$	0.089	0.017	0.026	0.026[a]	

Estimated accuracy (±)				
	ZnS	ZnTe	ZnSe	CdTe
s_{11}	0.2%	1%	2%	1.5%
s_{12}	0.5%	1%	2%	1.5%
s_{44}^E, s_{44}^D	0.2%	1%	3%	1.5%
d_{31}				
ϵ_{11}^T, ϵ_{11}^S	2%	2%	2%	2%
k_{14}	2%	4%	4%	4%
d_{14}	3%	5%	5%	5%
e_{14}	3%	6%	8%	6%

[a] Using ratios of values for ZnS at 25 and −196°C, these values are, respectively, 1.54, 0.030$_4$, and 0.023 at 25°C.
[b] See reference 8.

[21] R. Frerichs and W. Minkus, Report on Contract No. AF 33(616)–5625, 1960 (unpublished). This report indicates that $(\partial P/\partial\theta)_T$ is not constant with temperature for CdS, but the changes are not particularly pronounced.
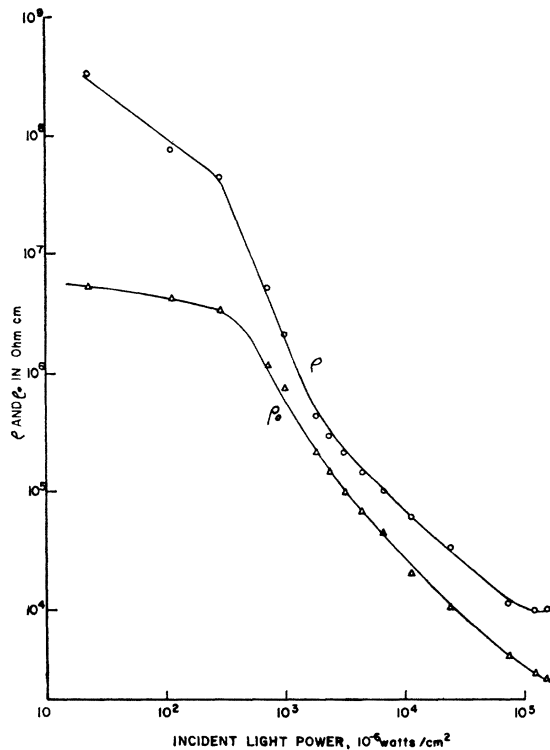
FIG. 1. ρ and ρ_0 for CdS vs perpendicular illumination.

step, this may be done from the elementary assumption that the atoms may be replaced by point charges of fixed value and that nearest-neighbor distances $AB=b$ (bond length) remain equal during elastic deformation. For the cubic (sphalerite) structure, this approach[23] may be applied to an elastic shear strain S_4 coupled with a relative displacement of the A and B sublattices normal to the plane of shear, and gives the relation

$$e_{14}=ne/d^2=(3/16)ne/b^2,\tag{7}$$

where ne is the effective charge of the atom and $d=4b/\sqrt{3}$ is the cubic lattice constant. Similar calculations may be made for the *ideal* hexagonal wurtzite lattice, in which each A atom is exactly at the center of a tetrahedron of B atoms and vice versa, just as in the sphalerite structure. The hexagonal lattice constants are then $c=8b/3$ and $a=(8/3)^{1/2}b$; a is the distance between nearest *like* atoms. We first consider a strain system S_3, $S_1=S_2=-\frac{1}{2}S_3$, that is, an elongation parallel to the hexagonal axis and a contraction of one-half the amount in the basal plane, resulting in zero volume change. All strains are small compared to unity, and terms in S^2 are disregarded. The piezoelectric charge density is then

$$D_3=e_{31}S_1+e_{31}S_2+e_{33}S_3=(e_{33}-e_{31})S_3.\tag{8}$$

The condition of equal nearest-neighbor distance de-

representing only 23 and 16% of the total pyroelectric effect.

C. Dependence of Mechanical Q on Photoconductivity in CdS

The variation of the effective dc volume resistivity[22] ρ vs incident light power for the CdS specimen is shown in Fig. 1. The effective resistivity $\rho_0=R_0lw/t$, where R_0 is given by the solution of Eq. (4), is also shown as function of incident light power. ρ_0 thus represents the effective volume resistivity at the antiresonance frequency. Figures 2 and 3 show the open-circuit mechanical Q as function of incident light power and ρ_0, respectively. The open-circuit Q, here associated with the elastic constant $s_{11}{}^D$, goes through a minimum as function of light intensity, as noted by Hutson.[3] For comparison, the short-circuit mechanical Q for CdS is 10 000.

IV. ELEMENTARY CALCULATION OF PIEZOELECTRIC EFFECTS FROM LATTICE DATA

The availability of measured piezoelectric constants for a number of AB compounds invites a new attempt to relate these constants to atomic structure. As a first
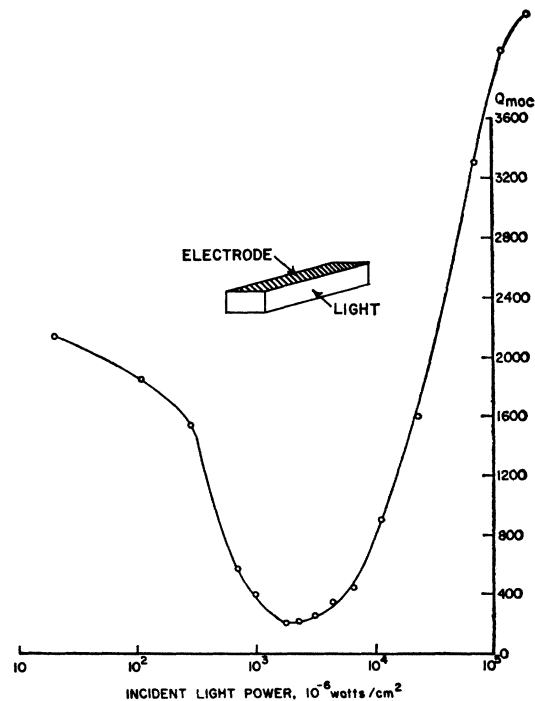

FIG. 2. Mechanical Q at antiresonance for CdS lateral expander bar vs light intensity. (Q_{MOC} calculated from resistance at resonance and antiresonance.)

---

[22] Most of the light which created the photoconductivity in this experiment is very highly absorbed by CdS, and the conductivity was, therefore, highest near the illuminated surface, hence the term "effective" volume resistivity.

[23] H. Jaffe, Phys. Rev. 66, 357 (1944).

mands that the strain S_3 be entirely provided by a change in the spacing of the AB double layer, since the vectors connecting the B atoms in one double layer to the A atoms of the next double layer remain parallel to the Z axis, which is still a sixfold symmetry axis under the particular strain system applied (Fig. 4). Application of the Pythagoras theorem to the triangle LMN (Fig. 4) before and after deformation shows that the prescribed lateral strain $S_1 = S_2 = -\frac{1}{2}S_3$ is present.

The calculation of the electric charge density D_3 of a system of double layers requires the fixing of a boundary condition for the whole crystal on the surfaces normal to the Z axis.[24] This is obtained from the requirement that the potential difference between these surfaces shall be zero before the crystal is strained. One may achieve this by placing single layers containing only one-fourth of the atoms at the two ends of the crystal, or by omitting one-fourth of the atoms from the outside half of the terminating double layers. The same result is obtained by assuming complete double layers and placing equal external charges of opposite sign on the end faces, such that they create a potential difference equal and opposite to that due to the summed potential steps in the double layers. Using the first approach, we have (Fig. 4)

$$D_3 = \tfrac{3}{4}NnecS_3/2, \qquad (9)$$

where N is the number of AB molecules per unit volume. The hexagonal unit cell of volume $\frac{1}{2}a^2c\sqrt{3}$ contains 2 molecules, whence

$$D_3 = \tfrac{1}{2}\sqrt{3}neS_3/a^2. \qquad (10)$$

Comparison of Eqs. (10) and (8) gives

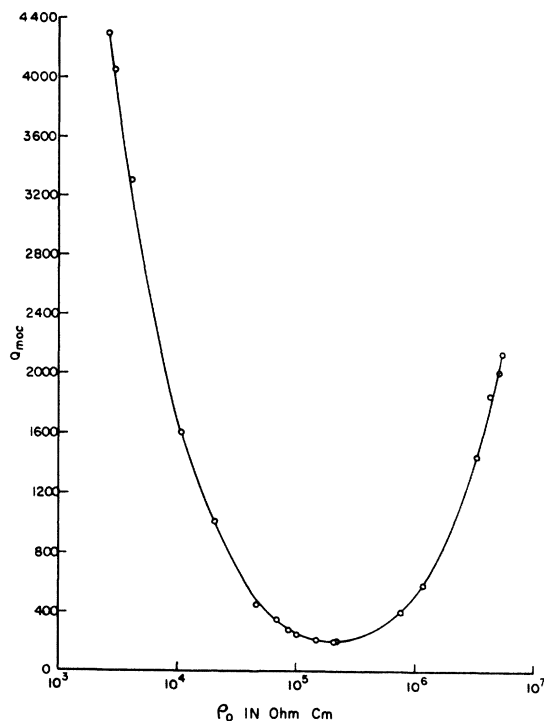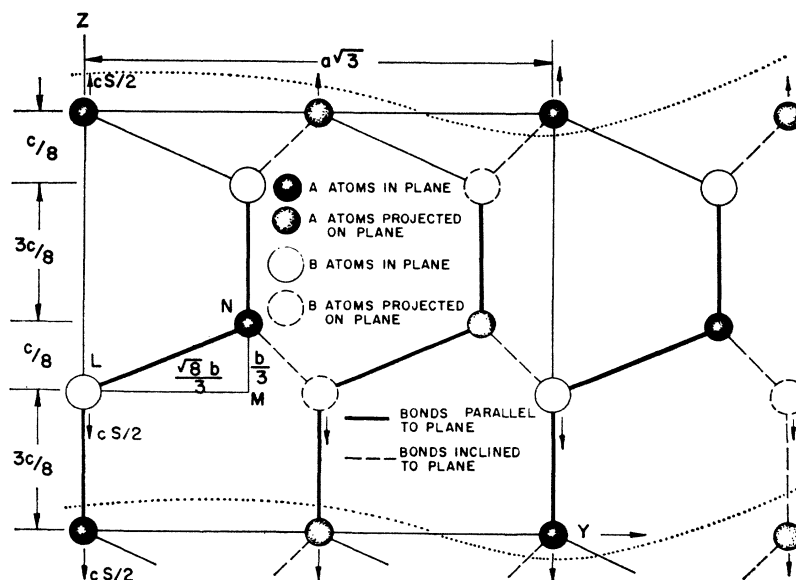$$e_{33} - e_{31} = +\sqrt{3}ne/2a^2 = +(3\sqrt{3}/16)ne/b^2. \qquad (11)$$

FIG. 3. Q_{MOC} vs ρ_0 for CdS transverse expander bar. (Q_{MOC} calculated from resistance at resonance and antiresonance.)

The positive sign here indicates that extension along Z gives positive charge on the A atom side of the double layer.

Next we consider an isotropic strain $S_1 = S_2 = S_3$, satisfied by an equal change of all bond lengths without change in bond angles, resulting in zero electric dis-

FIG. 4. Section through wurtzite lattice parallel to symmetry plane [parallel to hexagonal $c(Z)$ and normal to $a(X)$ axis]. Strain is entirely supplied by spacing change in two double layers of combined thickness one-fourth of unit cell height c. Curved lines indicate crystal boundaries for zero initial potential difference.

---

[24] This was not yet recognized in the abstract (reference 9) and the values for n in that abstract are partly incorrect.
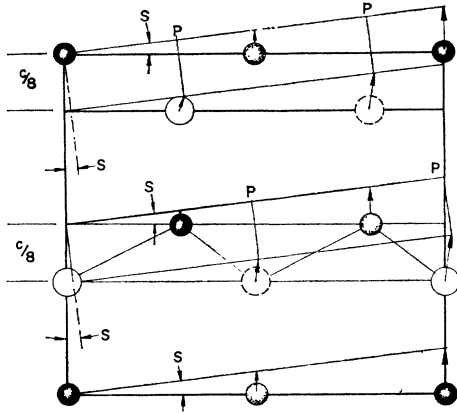
FIG. 5. Shear strain S_4 in symmetry plane of wurtzite lattice. Each double layer is rigidly rotated in respect to the c axis to satisfy equality of the bonds within the double layer.

TABLE VI. Effective atomic charge n on metal atom calculated from bond length b (in 10^{-10} m) and piezoelectric constants e (in C/m^2).[a]

	b		e_{14}	n	
Cubic					
ZnS	2.34		0.147	+0.268	
ZnSe	2.46		0.049	0.099	
ZnTe	2.64		0.0284	+0.066	
CdTe	2.81		0.031	0.081	

	b	r	e_{15}	n	$e_{33}-e_{31}$	n
Hexagonal						
ZnO[b]	1.98	0.0188	−0.5	1.1	1.8	1.3
CdS	2.53	0.0058	−0.210	+0.77	0.731	+0.90
CdSe	2.63	0.0041	−0.138	+0.55	0.507	+0.68

[a] $r = 1 - (3/8)^{1/2}c/a$ indicates deviation from ideal wurtzite structure.
[b] The values for e_{15} and $e_{33}-e_{31}$ were obtained using piezoelectric data of Hutson (see reference 3) and elastic data of T. B. Bateman [J. Appl. Phys. 33, 3309 (1962)].

placement:

$$D_3 = (2e_{31} + e_{33})S_1 = 0,$$

and (12)

$$e_{31} = -\tfrac{1}{2}e_{33}.$$

The effect of a shear strain S_4 in the YZ plane consists of a tilting of the AB double layers in respect to the Z axis (Fig. 5). Equality of the 3-dimensional bond framework inside the double layers requires the B atoms to remain on the normals at the centers P of equilateral triangles of A atoms in the tilted basal plane. This leads to a sidewise displacement of the B atoms relative to the A atoms of $S_4c/8$, resulting in electric displacement

$$D_2 = -NnecS_4/8 = -\sqrt{3}neS_4/6a^2, \qquad (13)$$

and

$$e_{15} = e_{24} = D_2/S_4 = -\sqrt{3}ne/6a^2 = -(\sqrt{3}/16)ne/b^2. \quad (14)$$

By comparison with Eqs. (11) and (12)

$$e_{15} = -\tfrac{1}{3}(e_{33} - e_{31}) = e_{31}. \qquad (15)$$

If our model of point charges is to retain the ideal wurtzite structure independent of temperature and hydrostatic pressure, symmetry permits only an isotropic change in lattice parameters as a result of temperature and pressure changes. The two thermal expansion coefficients must then be equal and the elastic constants satisfy

$$s_{11} + s_{12} = s_{33} + s_{13}. \qquad (16)$$

The resultant electric displacement is zero, hence the pyroelectric effect disappears, and the piezoelectric strain constants satisfy

$$d_h = d_{33} + 2d_{31} = 0. \qquad (17)$$

The preceding model considerations for the ideal wurtzite structure may also be applied to the sphalerite structure if the latter is referred to a trigonal [111]

axis (cube diagonal) as Z axis, because the two structures differ only by rotation of successive double layers around this axis. Indeed, if the elastoelectric matrix of the sphalerite class and Eq. (7) are transformed to this rotated coordinate system, Eqs. (11), (12), (15), (16), and (17) result, as well as the nonexistence of a pyroelectric effect. Landauer[25] derived a pyroelectric effect for the sphalerite lattice, but this paradoxical result is due to his failure to postulate zero potential difference before temperature change, as discussed above for stress application.

Equation (12) is well satisfied by e_{33} and e_{31} of CdS. For CdSe the deviation is probably within the limit of error of e_{33} and e_{31}. Equation (15) is only approximately fulfilled for both CdS and CdSe. This is expressed in alternate values for n in Table VI. It is noteworthy that Eq. (17) is satisfied by the experimental d constants of CdS and CdSe within their much closer tolerances, although it was derived from a more restricted model. The observed pyroelectric effect is small—the total change in moment from 77 to 300°K corresponds to only one-thousandth of the charge density of each layer and may well be related to temperature dependence of the deviation from ideal wurtzite structure, which also manifests itself in the observed anisotropy of thermal expansion. The elastic isotropy Eq. (16) is satisfied within 5% for CdS and CdSe.

Equations (7), (11), or (14) can be used to calculate the effective charge for our model. The results are given in Table VI, which also includes hexagonal ZnO for which approximate piezoelectric data are available.[3,12] By convention, the sign of the piezoelectric constant d_{33} is taken to be positive in all crystals of class 6 mm.[26] To obtain the sign of the effective charge on the A (metal) atoms from the piezoelectric data and the model theory, one must have an experimental connec-

[25] R. Landauer, J. Chem. Phys. 32, 1784 (1960).
[26] Standards on Piezoelectric Crystals, Proc. Inst. Radio Engrs. 37, 1387 (1949).

tion between the sign of d_{33} (hence, e_{33}) and the AB sequence in the double layer. This has been obtained by x-ray intensity measurements for ZnS,[27] CdS,[28] CdSe,[29] and ZnTe.[28,10] In each case, a positive electric charge appears on an extension parallel to the Z axis on the metal side of the double layers; from this fact, our theory derives the positive charge of the metal atoms.

The values for effective charge n in Table VI show increasing polarity with increasing weight of the metal atom, Zn, Cd, and decreasing weight of the nonmetal, Te, Se, S, and O. These sequences conform with the general chemical rule that electronegativity decreases with increasing atomic number in each column of the periodic system, although it is of interest that Pauling[30] finds Cd to be slightly more negative than Zn on the basis of thermochemical data. If we accept the point of view that a tetrahedrally bonded fully covalent crystal would have two negative charges on the metal atom,[31] even the most weakly piezoelectric crystal studied, ZnTe, is found to be more than 50% ionic since n (Table VI) is still positive.

V. CONCLUSIONS

The elastic data for the six II–VI compounds reported in this paper show great similarity with little distinction between the sphalerite and wurtzite structures[32] as shown by Table VII. The level of compliance increases smoothly with atomic number of both A and B atoms. The piezoelectric constants for the wurtzite-type crystals nearly satisfy the symmetry requirements of the cubic sphalerite type, but have much higher magnitude. We believe that the stronger piezoelectricity and the preference for the wurtzite structure are both direct consequences of increasing ionicity of the bond.

TABLE VII. Short-circuit elastic constants normalized to $s_{11}{}^E$.

| | Cubic–Rotated | | Cubic–Rotated | | Hexagonal | |
	ZnS	ZnTe	ZnSe	CdTe	CdS	CdSe
s_{12}/s_{11}	−0.42	−0.38	−0.41	−0.46	−0.48	−0.48
s_{13}/s_{11}	−0.20	−0.20	−0.15	−0.26	−0.28	−0.245
s_{33}/s_{11}	0.78	0.82	0.74	0.80	0.81	0.74
s_{44}/s_{11}	3.72	3.47	3.95	3.70	3.20	3.24
s_{66}/s_{11}	2.84	2.76	2.82	2.92	2.96	2.96
s_{14}/s_{11}	0.62	0.50	0.73	0.56	0	0

The effective charges derived from the piezoelectric data appear reasonable. A quantitative theory should be based on lattice dynamics including nearest-neighbor repulsive forces, atom polarizability, and long-range forces, in addition to the Coulomb interactions. Bond-angle-dependent forces will also be substantial in partly covalent tetrahedral structures. Theoretical efforts in some of these directions include those of von Hippel,[33] Birman,[34] Tolpygo,[35] and especially Cochran.[36] The break in the level of piezoelectric constants between the hexagonal and cubic crystals indicates the limited validity of the present geometric theory. It seemed worthwhile, however, to show that a purely geometric consideration produces results of the right order of magnitude and a reasonable chemical sequence.

ACKNOWLEDGMENTS

[27] D. Coster, K. S. Knol, and J. A. Prins, Z. Physik **63**, 345 (1930).
[28] W. R. Cook, Jr. (private communication).
[29] R. Zare, W. R. Cook, Jr., and L. R. Shiozawa, Nature **189**, 217 (1961).
[30] L. Pauling, *The Nature of the Chemical Bond* (Cornell University Press, Ithaca, New York, 1960), 3rd ed., p. 93.
[31] L. Pauling, reference 30, p. 246.
[32] V. A. Zhdanov and L. Brysneva, Soviet Phys.—Cryst. **6**, 514 (1962) have recognized this for ZnS and CdS.

[33] A. von Hippel, Z. Physik **133**, 158 (1952).
[34] J. L. Birman, Phys. Rev. **111**, 1510 (1958).
[35] K. B. Tolpygo, Fiz. Tverd. Tela **2**, 2655 (1960) [translation: Soviet Phys.—Solid State **2**, 2367 (1961)].
[36] W. Cochran, in *Advances in Physics*, edited by N. F. Mott (Taylor and Francis, Ltd., London, 1961), Vol. 10, p. 401.